Journal of Al-Azhar University Engineering Sector

Vol. 19, No. 72, July 2024, 858-877

MINIMUM REINFORCEMENT REQUIRED FOR CONCRETE BEAMS WITH HYBRID BARS AND HYBRID FIBERS-NUMERICAL INVESTIGATION

Ahmed E. Ewis, Mohamed H. Makhlouf *, Ahmed H. Abdel-Karim, Gamal I. Khalil

Civil Department, Faculty of Engineering, Benha University, Benha, 13518, Cairo, *Egypt*.

***Correspondence:** mohamedmakhlouf83@yahoo.com

Citation:

A.E. Ewis, M.H. Makhlouf, A.H. Abdel-Karim, and G.I. Khalil, "Minimum Reinforcement Required for Concrete Beams with Hybrid Bars and Hybrid Fibers-Numerical Investigation", Journal of Al-Azhar University Engineering Sector, vol. 19, pp. 858 - 877, 2024.

Received: 3 December 2023

Revised: 12 January 2024

Accepted: 31 January 2024

DOI:10.21608/auej.2024.256569.1541

ABSTRACT

The intent of this research is to establish a design procedure and formulate equations for a novel construction material. Adhering to design codes, one crucial requirement is to verify the minimum reinforcement area to ensure the ductile failure of RC members and mitigate crack formation resulting from shrinkage. Within this study, the authors explore the minimum reinforcement of beams with both hybrid bars and hybrid fibers through the utilization of numerical simulations. To analyze the flexural behavior of low reinforcement ratio members, fifteen RC beams are modeled and subjected to four-point loading configurations. The parameters under scrutiny encompass the hybrid reinforcement ratios ranging from 0.0% to 0.50%, as well as the beam depth. The outcomes of the numerical analysis, obtained through the Nonlinear Finite Element Analysis (NLFEA) method, are presented in light of maximum deflection, and cracking and peak capacity. Two distinct approaches are employed to explore the minimum reinforcement ratios: (a) the cracking moment approach and (b) the Ductility Index (DI) approach. Comparative evaluations between these approaches demonstrate that the incorporation of hybrid fibers allows for a reduction in the minimum reinforcement ratio. Specifically, when implementing the DI approach, the minimum reinforcement ratio decreases to 0.081% instead of 0.18% for RC beams. Notably, the DI approach exhibits superior agreement with the NLFEA results in comparison to the cracking moment approach.

KEYWORDS: Hybrid bars, Hybrid fibers, minimum reinforcement ratio, ductility index approach, cracking moment approach.

نسب الحديد الدنيا المطلوبة للكمرات الخرسانية المسلحة بألياف الفايبر الهجين وأسياخ التسليح الهجين

أحمد السيد عويس، محمد حسين مخلوف*، أحمد حسن عبدالكريم، جمال إسماعيل خليل

قسم الهندسة المدنية، كلية الهندسة ببنها، جامعة بنها، 13518، القاهرة، مصر.

***البريد الاليكتروني للباحث الرئيسي :** mohamedmakhlouf83@yahoo.com

الملخص

الهدف من هذا البحث هو إنشاء منحنيات وصياغة معادلات لتصميم العناصر الخرسانية ذات مواد البناء الحديثة. واحدة من المتطلبات الأساسية في الامتثال لشروط التصميم هي التحقق من الحد الأدنى لنسبة التسليح لضمان وجود انذارات قبل انهيارالعناصرالخرسانية المسلحة والتخفيف من تكوين الشروخ الناتجة عن الانكماش. في هذه الدراسة، يقوم الباحثون بدراسة التسليح الأدنى للكمرات المسلحة بأسياخ مهجنة بالاضافة إلي وجود ألياف الفايبر من خلال استخدام المحاكاة العددية. تم نمذجة وتحليل خمسة عشر كمرة خرسانية مسلحة لفهم ومعرفة سلوك الانحناء للكمرات

ذات نسبة تسليح منخفضة. وتشمل المتغيرات المدروسة نسب التسليح التي تتراوح بين 0.0% و0.5%، بالإضافة إلى تغيير عمق الكمرات. وتُصنف نتائج التحليل العددي التي تم الحصول عليها في ضوء الترخيم الكلي للكمرات، عزوم التشرخ وعزوم الانحناء القصوي. تُستخدم طريقتين مختلفتين لايجاد نسبة التسليح الدنيا: (أ) طريقة عزوم التشرخ و (ب) طريقة معامل الممطولية. وتظهر التقييمات المقارنة بين الطريقيتين أن استخدام الألياف الهجين يسمح بتقليل نسبة التسليح الأدنى. على وجه الخصوص عند تطبيق طريقة معامل الممطولية، تنخفض نسبة التسليح الأدنى إلى 0.081% بدلاً من 0.18% للكمرات المسلحة . جدير بالذكر أن طريقة معامل الممطولية يظهر توافقًا أفضل مع نتائج التحليل العددي مقارنة بطريقة عزوم التشرخ.

الكلمات الدالة : أسياخ التسليح الهجين، الفايبر الهجين، أدني نسبة تسليح، طريقة معامل الممطولية، طريقة عزوم التشرخ.

1. INTRODUCTION

In recent decades, there has been a growing general trend for countries to construct tourism cities, ports, and factories in coastal areas and near the sea. This vision has posed challenges for researchers and construction professionals who seek long-term durability in such environments. Traditional construction materials are often inadequate for these structures. One of the critical concerns is the corrosion of reinforcing steel, which not only reduces the service life of buildings but also necessitates frequent maintenance cycles during construction [1, 2]. Furthermore, evaluating the performance of corroded reinforced concrete (RC) structures against lateral loads is complex and demands substantial effort to assess the effectiveness of strengthening and upgrading methods [1]. Extensive research has been conducted to explore various solutions suitable for corrosive environments [3]. These solutions include galvanized steel, and polymer-impregnated concrete epoxy coatings. As a substitute for traditional steel bars, fiber-reinforced polymer (FRP) reinforcing bars have emerged as a viable option [4, 5]. The utilization of FRP bars in concrete structures exposed to aggressive environments helps extend their service life and reduces life cycle cost [3, 6]. Their innovative properties, such as lightness, corrosion resistance, electromagnetic transparency, and high tensile strength made FRP composites employed in various applications in different industries [7]. However, FRP bars are still restrictedly employed in the construction field. Despite the various advantages it offers, the utilization of FRP rebar as a tensile reinforcement is limited due to several reasons. These include its low modulus of elasticity, which affects its stiffness compared to traditional reinforcing steel. Additionally, FRP rebar is susceptible to brittle failure, which can impact its structural performance. Another factor limiting its use is the relatively higher cost of FRP rebar compared to traditional reinforcing steel. These factors contribute to the restricted adoption of FRP rebar as a preferred reinforcement material in certain applications [8].

Owing to FRP bar shortcomings and steel bar corrosion problems, there are two strategies to overcome these issues. The first strategy is utilizing ductile reinforcement bars or hybrid schemes. Many studies have been conducted for the fabrication of ductile or pseudo-ductile bars that combined corrosion resistance and failed in a ductile manner [9]. Hybrid bars divided into four series fabricated from different materials (Carbon-Basalt, steel wires – Basalt fibers with two volume fractions, and steel bar-basalt fibers) have been investigated. Test results revealed that bars fabricated from steel wires and basalt fibers have a higher energy absorption compared to other studied bars. Moreover, the elasticity modulus and tensile resistance capacity improved by 83% to 120% and 6% to 26%, respectively, compared to GFRP bars [10]. Also, hybrid GFRP bars with steel wires were fabricated and utilized as tensile reinforcement for six high-strength concrete beams. The studied parameter was the reinforcement type (steel, GFRP, and hybrid GFRP). Test results showed that hybrid GFRP-reinforced beams exhibit ductile deformation similar to steel-reinforced beams [11]. Hybridization schemes refer to utilizing FRP bars at the outer level of the tension zone and steel bars at the inner level to provide higher corrosion resistance. For example, variation of reinforcement ratio (AF/As) of eight beams with a hybridization scheme reinforcement bar of (steel-GFRP) were studied [12]. It is reported that no impact was recorded for the difference in axial stiffness between reinforcement on the ultimate capacity. In the other side, increasing the reinforcement ratios showed an essential effect

in the ductility response.

The second strategy is the employe of non-metallic fibers in concrete mixtures like polypropylene fibers (PP), polyethylene fibers (PE), polyolefin fibers (PF), and polyvinyl alcohol fibers (PVA) which become widely available in the local market. The fibers' role in reinforced concrete structures could be classified in two ways: (a) resisting a portion of the tensile stress in the tension zone; (b) improving the bond between the mixture and the reinforcing bars [13]. The addition of fibers helps increase the ultimate flexural capacity and the maximum deflection, as reported by [14, 15]. Moreover, fibers could reduce the crack width by reducing the stress in reinforcing bars, as investigated [16]. As well, Bernard reported that the inclusion of synthetic fibers improved the serviceability performance in terms of crack width [17]. Also, the inclusion of fibers could result in better toughness and post-cracking responses of concrete members [18-19]. However, utilizing single fiber in concrete mixtures limits crack arrest depending on the type of fiber used. Therefore, fiber hybridization by combining different types of fiber in one mixture is more effective and is known as hybrid fiber reinforced concrete (HyFRC) [13]. The flexural response of RC beams includes steel and polypropylene fibers has been studied [20]. The test results approved an increment in the range of 25 to 100% in the flexural capacity due to using hybrid fibers compared to plain concrete. Abadi et al. investigated the result of hybrid fibers (steel and micro or macro polypropylene fibers) inclusion on beam performance under static loads. Fiber's addition and volume fraction ratios were the main parameters studied. It was reported that the hybrid fiber system helps in decreasing the mid-span deflection, reducing the steel reinforcement bars strain, and reducing the crack width [21].

Coastal buildings include many lightly reinforced structural elements that require reinforcement area that cannot be lower than the minimum reinforcement area. In lightly reinforced concrete (LRC) structures, it becomes imperative to establish a precise definition for the minimum reinforcement ratio ρ_{min}. This parameter assumes paramount importance as it serves the dual purpose of meeting both the ultimate strength and serviceability requirements of the structure. [22]. For high-strength concrete, the effect of the inclusion of fibers on the minimum reinforcement ratio has been investigated [23]. Eighteen beams were tested to explore the effect of the type and volume fraction of fibers and the reinforcement ratio on the flexural behavior. Test results revealed that the minimum reinforcement ratio calculated using ACI 318-08 [24] may be re-evaluated based on concrete tensile properties. There are several variables affecting the minimum reinforcement ratio, for instance concrete compressive strength and the yield strength of tensile reinforcement which are the primary key for define the minimum reinforcement based on design codes (ACI 318, Eurocode 2) [24, 25]. The Canadian standard (CSA A23.3-04) [26] definition was based on the relation between concrete cracking moment and the moment capacity of tensile reinforcement. Some studies investigate the impact of beam height on flexural ductility. For example, the effect of beam height on the member's ductility and concluded that increasing the beam depth results in decreasing the beam ductility has been investigated [27]. In addition, other studies reported that larger beams failed in a brittle manner rather than smaller beams [28-31]. Also, the influence of beam height was investigated experimentally and numerically in an extensive test project [32]. It is worth mentioning that the beam height affects the minimum reinforcement area.

The minimum fiber dosage $V_{f,min}$ in fiber-reinforced concrete beams (FRC) can be defined similar to ρ_{min} for LRC beams [33-35]. In some cases, the utilization of fibers and reinforcement bars could be provided together in a single beam, known as hybrid reinforcement concrete beams (HRC). If the evaluation of minimum reinforcement in HRC beams is conducted similarly to that of LRC beams, the potential benefits of fiber as a reinforcement are not utilized. Consequently, the inclusion of fiber reinforcement becomes ineffective in enhancing structural performance. The effect of volume fraction of the fiber used on the mechanical behavior of FRC beams and corresponding

influence on their failure modes (ductile or brittle) has been studied [33]. The study evaluated the minimum fiber dosage required to shift the failure from brittle to ductile similar to minimum reinforcement ratio. A new approach has been defined in terms of ductility index and results revealed ductile mode could be achieved when DI value is positive. Also, the design of FRC tunnel segments following the requirements of Model code (MC) 2010 has been studied [33]. The study simulated numerically the segment used in Barcelona metro station. This study proposed an approach for the required fibers with relation to accidental eccentricity (e). Compared with MC 2010, the new approach reduces the required fiber for tunnel segment without loss of quality during the station service life by 25%.

The combination of fibers and reinforcement in the application of tunnel lining has been investigated [36]. The study reported that steel fibers can resist tensile stresses and the minimum reinforcement in design codes could be minimized. This is especially evident in the context of large-scale structures when the computation of the minimum steel reinforcement, as per building code regulations, results in a substantial quantity of steel rebar.

The assessment of the literature has reported that aforementioned studies and codes concentrated on the factor effects on the minimum reinforcement of RC beams. Furthermore, limited investigations have studied the result of the inclusion of fibers on the minimum reinforcement ratio [22, 37]. Based on the previous work of the authors, which involved conducting tests and numerical analyses on 14 concrete beams reinforced with hybrid fibers and reinforcement bars (steel, GFRP, and hybrid), as reported in another publication [38], the present study aims to provide a numerical investigation for the minimum hybrid reinforcement by change the reinforcement ratio and beam depth.

2. Finite Element Method

Within this section, a numerical simulation using the ABAQUS/CAE 2020 software package was performed to examine the flexural response of beams with different reinforcement bars and hybrid fibers. The simulations were conducted using Nonlinear Finite Element Analysis (NLFEA) to replicate the experimental response of the tested beams. Numerous factors were considered during the modeling process, including the selection of element types, material properties, assembly of components, step definitions, interactions between parts, loading conditions, and types of supports. Comparing the results obtained from the experimental tests with those generated by the simulations serves as an effective method to validate the finite element (FE) models accuracy.

2.1. Geometry Model

The experimental setup for the structural component was replicated in ABAQUS using various types of structural elements. The concrete part was represented with a C3D8R solid element, while the top, bottom reinforcement and stirrups were modeled using T3D2 truss elements. The supporting and loading cylindrical parts were represented using rigid elements. The simulation assumed a complete bond between the embedded reinforcement and the concrete. The analysis of the model followed the displacement control loading method. **Fig. 1** illustrates the three-dimensional simulation model of one of the tested beams.

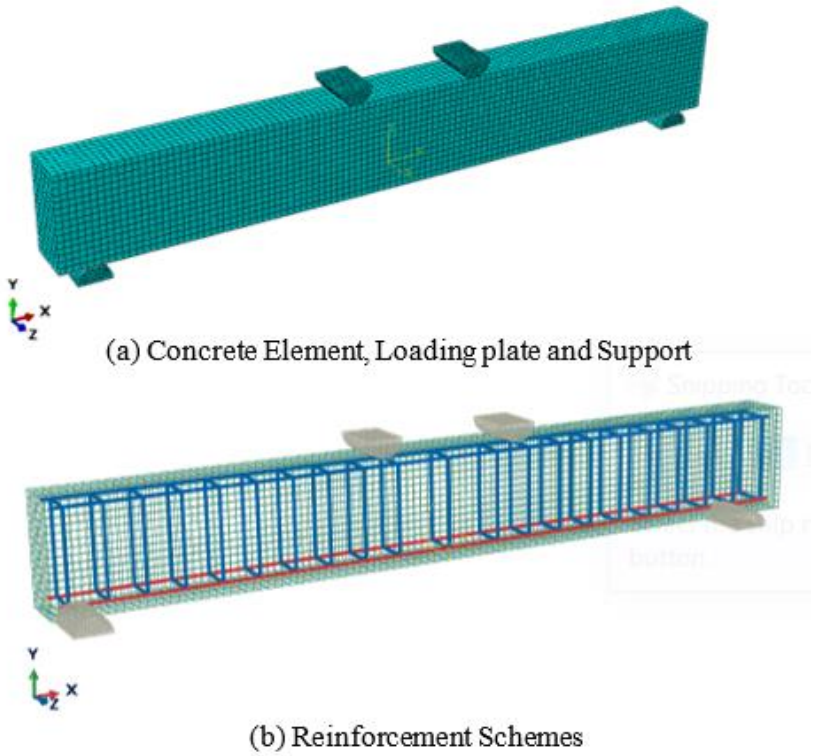

Fig. 1. Representation of Tested Beam.

2.2. Concrete behavior Modelling in compression

The Wight MacGregor model [39] was utilized to define the compressive stress-strain relationships of concrete. The parameters definition of the concrete damage plasticity (CDP) model for hybrid fiber concrete (HyFRC) were based on the developed equations by Zainal et al. [40] and are depicted in **Fig. 2**. The following equations were used to determine these parameters:

$$\sigma_c = (1 - d_c)E_0(\varepsilon_C - \varepsilon_C^{pl,h}) \quad \text{Eq. (1)}$$

$$\varepsilon_C^{in,h} = \varepsilon_C - \frac{\sigma_C}{E_O} \quad \text{Eq. (2)}$$

$$\varepsilon_C^{pl,h} = \varepsilon_C - \frac{\sigma_C}{E_O}\left(\frac{1}{1-d_c}\right) \quad \text{Eq. (3)}$$

$$\varepsilon_C^{pl,h} = \varepsilon_C^{in,h} - \frac{\sigma_C}{E_O}\left(\frac{d_c}{1-d_c}\right) \quad \text{Eq. (4)}$$

Furthermore, in this study, the Kent and Park [41] were described the model for unconfined concrete behavior .This model is commonly represented by the following equation:

$$`\sigma_c = \sigma_{cu}\left[2\left(\frac{\varepsilon_c}{\varepsilon_c'}\right) - \left(\frac{\varepsilon_c}{\varepsilon_c'}\right)^2\right] \quad \text{Eq. (5)}$$

where σ_c and σ_{cu} are the nominal and ultimate compressive stress, ε_c and ε_c' are the nominal and ultimate compressive strain, respectively, E_o is the modulus of elasticity, $\varepsilon_C^{in,h}$ the elastic hardening strain in compression, and $\varepsilon_C^{pl,h}$ is the plastic hardening strain in compression.

The computation of compression damage parameter, d_c, may be achieved using the below equation:

$$d_c = 1 - \frac{\sigma_c}{\sigma_{cu}} \quad \text{Eq. (6)}$$

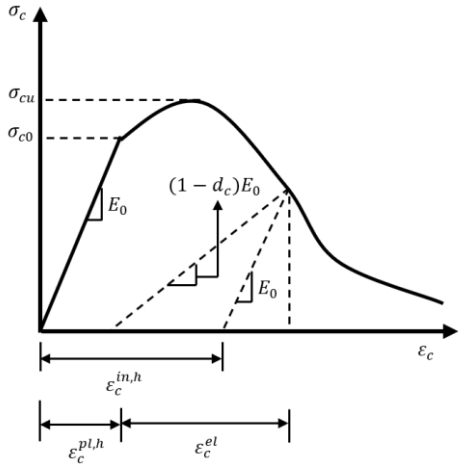

Fig. 2. Definition of concrete behavior for CDP Model in compression.

2.3. Concrete behavior Modelling in tension

The uniaxial tensile stress-strain behavior of concrete is simulated with Zainal et al. model [40], which is depicted in **Fig.3**. The plasticity hardening strain in tension, $\varepsilon_t^{pl,h}$, is determined based on the following equations:

$$\sigma_t = (1-d_t)E_0(\varepsilon_t - \varepsilon_t^{pl,h}) \quad \text{Eq. (7)}$$

$$\varepsilon_t^{ck,h} = \varepsilon_t - \frac{\sigma_t}{E_O} \quad \text{Eq. (8)}$$

$$\varepsilon_t^{pl,h} = \varepsilon_t - \frac{\sigma_t}{E_O}\left(\frac{1}{1-d_t}\right) \quad \text{Eq. (9)}$$

$$\varepsilon_t^{pl,h} = \varepsilon_C^{ck,h} - \frac{\sigma_t}{E_O}\left(\frac{d_t}{1-d_t}\right) \quad \text{Eq. (10)}$$

where σ_t and σ_{to} are the nominal and ultimate tensile stress, ε_t is the nominal and ultimate compressive strain, respectively, E_o is the modulus of elasticity, $\varepsilon_t^{ck,h}$ the elastic hardening strain in tension, and $\varepsilon_t^{pl,h}$ is the plastic hardening strain in tension.

The models computed the tensile strength σ_{t0} equal to 7–10% of maximum compressive strength σ_{cu}. The tensile damage could be expressed as follow:

$$d_t = 1 - \frac{\sigma_t}{\sigma_{to}} \quad \text{Eq. (11)}$$

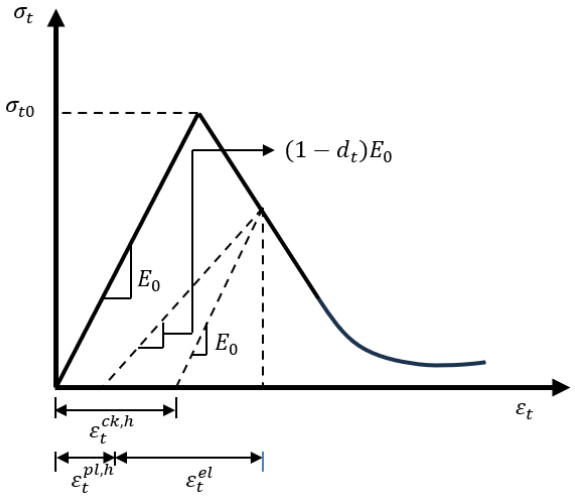

Fig. 3. Definition of concrete behavior for CDP Model in tension.

2.4. Reinforcement Modelling

The developed hybrid bar of 14 mm was fabricated using a 10 mm steel bar and the outer shell from glass fiber and resin as shown in Fig. 4. The mechanical properties of the hybrid bar are presented in Table 1. The behavior of hybrid bars under tensile force could be described in three stages: (i) the steel bar start yielding first; (ii) the outer glass fiber layers start to deform following by rupture of glass fiber; and (iii) the bar strength reduced gradually up to the steel bar damage. The stress-strain curve depicted in Fig. 5 was employed to define the properties of hybrid bars in the idealized form based on the tensile test results obtained by the authors in [38].

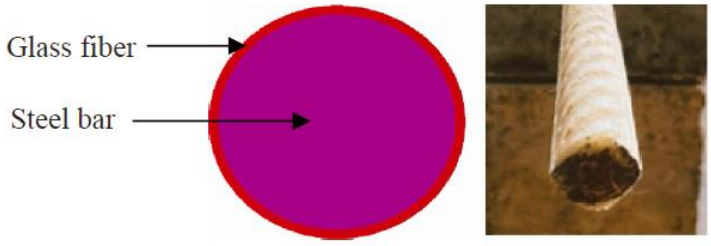

Fig. 4. Schematic view and actual specimen of hybrid bar.

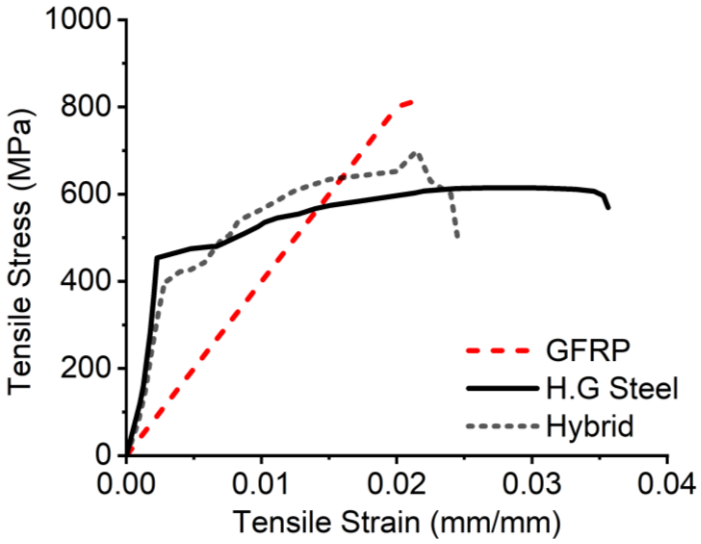

Fig. 5. Tensile stress versus strain relationship of hybrid bars in comparison with GFRP and steel bars.

Table 1. Mechanical properties of reinforcing bars.

Bar Types	Diameter (mm)	Modulus of Elasticity E (GPa)	Yield Strength (MPa)	Tensile Strength (MPa)
Hybrid	14	140	396	700

2.5. Comparison between Experimental and NLFE model

To validate the numerical model, the results obtained from the nonlinear finite element (NLFE) model were compared with the experimental data. This comparison primarily focused on

four categories: the failure modes, load versus deflection behavior, first cracking load, and ultimate capacity. The authors have documented the validation of the numerical model in their study [38].

3. Parametric Analysis

After validating the nonlinear finite element (NLFE) model using previous experimental results, as discussed earlier, the calibrated NLFE model is applied to further study the impact of certain parameters on the minimum reinforcement ratio. The following parameters are considered in this study: (a) Different beam depths: Two beam depths are examined, namely h = 300 mm and h = 450 mm. The beam width (b = 150 mm) and the depth-to-span ratio (h/L = 0.15) are kept constant. **Fig. 6** and **Table 2** illustrates the dimensions of the specimens and the arrangement of reinforcement; (b) Variation in reinforcement ratio (ρ) was in range from 0% to 0.5% of the cross-sectional area of each beam.

By analyzing these parameters using the calibrated NLFE model, the study aims to determine their influence on the minimum reinforcement ratio.

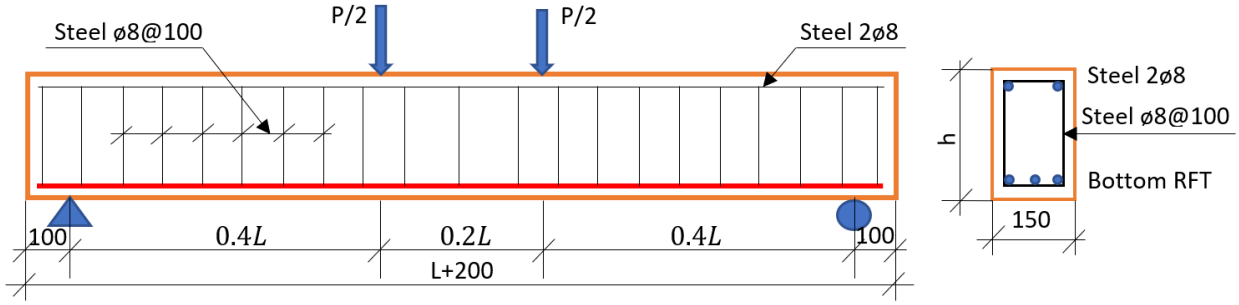

Fig. 6. Geometry and Reinforcement arrangement of Specimens used in parametric study

Table 2. Parametric study details.

Group	Beam	Cross-section (mm)		Fiber dosage ratio %			Tension RFT	
		b	h	V_{PP}	V_{MS}	V_t	Quantity	ρ %
Group A	A1	150	300	1.0	1.0	2.0	-	-
	A2	150	300	1.0	1.0	2.0	2ø3	0.031
	A3	150	300	1.0	1.0	2.0	2ø4	0.055
	A4	150	300	1.0	1.0	2.0	2ø5	0.087
	A5	150	300	1.0	1.0	2.0	2ø6	0.125
	A6	150	300	1.0	1.0	2.0	2ø7	0.171
	A7	150	300	1.0	1.0	2.0	2ø8	0.223
	A8	150	300	1.0	1.0	2.0	2ø10	0.349
	A9	150	300	1.0	1.0	2.0	2ø12	0.502
Group B	B1	150	450	1.0	1.0	2.0	-	-
	B2	150	450	1.0	1.0	2.0	2ø3	0.021
	B3	150	450	1.0	1.0	2.0	2ø4	0.037
	B4	150	450	1.0	1.0	2.0	2ø5	0.058
	B5	150	450	1.0	1.0	2.0	2ø6	0.083
	B6	150	450	1.0	1.0	2.0	2ø7	0.114
	B7	150	450	1.0	1.0	2.0	2ø8	0.149

4. Theoretical Models and Discussions

In certain conditions and architectural requirements, beams may be constructed with larger dimensions than necessary for their ultimate flexural strength. In such instances, it is crucial to provide minimum reinforcement to prevent the sudden failure of these beams [35]. The minimum reinforcement ratio prescribed in design codes is determined based on the approach that cracks occur in the flexural zone when the extreme tension fiber stress reach the concrete tensile strength (f_r). Once the beam section cracks in tension, the crack propagates towards a point close to the section's centroid, leading to a sudden tensile force transfer from the concrete to the reinforcement. At this point, the beam will display a ductile response if the reinforcement can withstand a moment capacity (M_d) greater than the cracking moment (M_{cr}) [36]. Studies have shown that the presence of fibers in reinforced concrete (RC) sections enhances the tensile resistance of concrete and assists a portion of the applied force [32]. Consequently, incorporating fibers can potentially reduce the minimum reinforcement required as stipulated in design standards and codes [22]. Researchers have proposed three approaches to compute the minimum reinforcement area in RC beams: (a) an approach linked to the cracking moment (M_{cr}), (b) an approach related to the ductility index (DI), and (c) an approach based on the brittleness number (N_p).

4.1. Nonlinear Finite Element Analysis (NLFEA) Results

Figure 7. illustrate the load-deflection relationship for each beam group, categorized into two groups (A and B). It has been reported that specimens with reinforcement below the minimum reinforcement ratio experience brittle failure, which could be expressed as the cracking load being lower than the ultimate loads. **Table 3** presents a comparison between the theoretical results and the results obtained from the nonlinear finite element analysis (NLFEA).

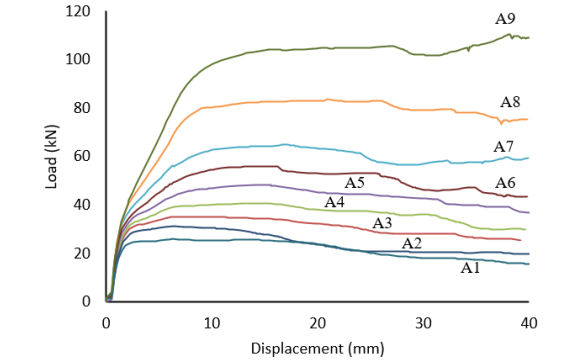

(a)

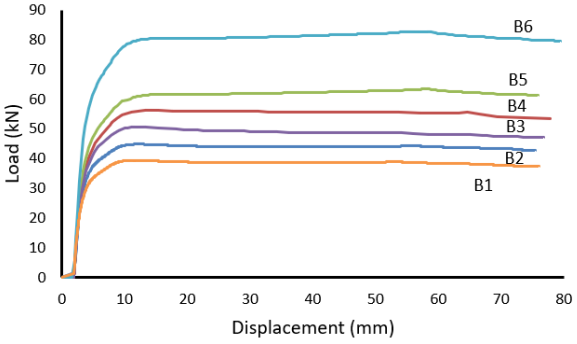

(b)

Fig. 7. Load-deflection curves for (a) Group A specimens, (b) Group B specimens

Table 3. NLFEA Parametric Study Results.

Group	Beam	Cracking Load kN	Peak Load kN	Maximum Deflection mm	Failure Case*
Group A	A1	24.08	25.92	6.28	Brittle
	A2	29.2	31.18	6.42	Brittle
	A3	29.46	35.18	7.64	Brittle
	A4	29.96	40.62	14.31	Ductile
	A5	34.91	48.16	15.55	Ductile
	A6	34.91	55.76	16.23	Ductile
	A7	36.63	65.91	18.21	Ductile
	A8	39.5	85.64	26.43	Ductile
	A9	41.45	110.42	38.52	Ductile
Group B	B1	39.46	37.56	11.03	Brittle
	B2	44.89	42.84	11.83	Brittle
	B3	43.22	50.75	11.88	Ductile
	B4	43.22	56.26	15.37	Ductile
	B5	50.89	63.48	58.05	Ductile
	B6	50.89	82.81	60.04	Ductile

*The failure mode was based on ductility index (DI) of each specimen compared with code DI

4.2. Minimum Hybrid Reinforcement Based on the cracking Moment approach (M_{cr})

With reference to the brittle failure condition, which indicates that beams fail in a brittle manner when the cracking moment (M_{cr}) is equal to or greater than the reinforcement yielding moment (M_y) as shown in **Fig. 8** [32].

The governing condition for the minimum percentage of hybrid reinforcement bars can be expressed as:

Strength of hybrid-reinforced concrete beams ≥ Strength of plain concrete beams - Additional strength due to hybrid fibers.

$$M_{n-hr,bars} \geq M_{cr-PC} - \Delta M_{cr,hr-fiber} = M_{cr,f} \quad \text{Eq. (12)}$$

$$A_{hr,min}\, f_{hr,bar}\, (d - \frac{a}{2}) = \frac{f_r\ I_g}{y_t} - \frac{R_{e,3}}{100}\frac{f_r\ I_g}{y_t} = (1 - \frac{R_{e,3}}{100})\frac{f_{r,min}\ I_g}{y_t} \quad \text{Eq. (13)}$$

where $A_{hr,min}$ is the minimum reinforcement area of hybrid bars, $f_{hr,bar}$ is the tensile strength of hybrid bars, d is the effective depth, a is depth of the rectangular stress block, $R_{e,3}$ is the residual tensile factor.

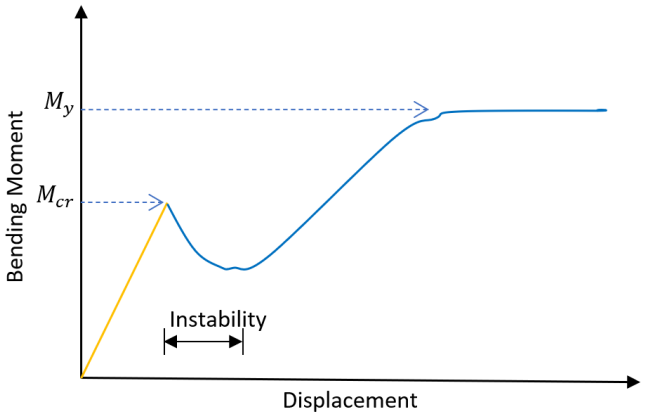

Fig. 8. Unstable load-displacement curve after cracking moment

Legeron and Paultre [42] reported a relation to estimate the modulus of rupture of concrete f_r as follows:

$$f_{r,min} = 0.68\sqrt{f_c'} \quad \text{Eq. (14)}$$

$$f_{r,avg} = 0.94\sqrt{f_c'} \quad \text{Eq. (15)}$$

$$f_{r,max} = 1.20\sqrt{f_c'} \quad \text{Eq. (16)}$$

This study used the chart shown in **Fig. 9** to estimate the tensile strength of concrete in relation to the reinforcement ratio. This chart has been developed based on the other studies experimental results involved in **Table 3**.

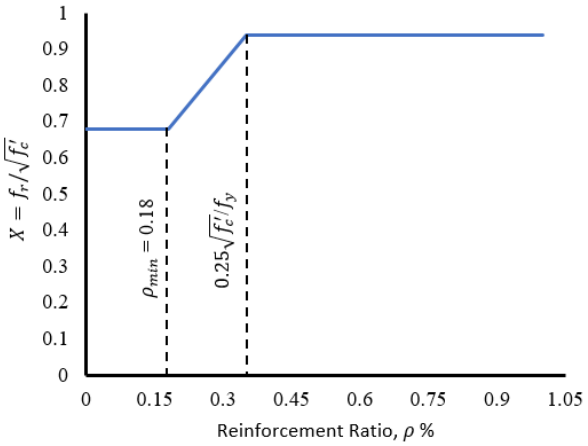

Fig. 9. Relation between reinforcement ration and modulus of rupture

The addition of fibers enhances the tensile strength of concrete, and the modulus of rupture of fiber concrete could be estimated using the following equation:

$$f_{r,fiber} = \left(1 + \frac{R_{e,3}}{100}\right) X \sqrt{f_c'} \quad \text{Eq. (17)}$$

where X is the factor that could be obtained from **Fig. 9**, and the residual strength factor ($R_{e,3}$) which could be obtained from the fracture test of notched FRC prism (150x150x500 mm) as per EN 14651-2005 [43]. In this study, the impact of hybrid fiber inclusion on the tensile resistance could be obtained from the splitting tensile test. The increases in tensile strength of 1% HyFRC and 2% HyFRC were 18% and 39%, respectively.

The gross moment of inertia (I_g) and the distance from extreme tension to the neutral axis (y_t) of the uncracked rectangular section may be computed ignoring the presence of hybrid bars and hybrid fibers for simplicity as follows:

$$I_g = \frac{bh^3}{12} \quad \text{Eq. (18)}$$

$$y_t = \frac{h}{2} \quad \text{Eq. (19)}$$

Substituting the values of I_g and y_t (equal to $bh^2/6$, for rectangular section) and f_r in Equation (14), we get,

$$\Phi M_{cr,f} = \left(1 - \frac{R_{e,3}}{100}\right) * 0.114\, bh^2\sqrt{f_c'} \quad \text{Eq. (20)}$$

In rectangular section, d/h usually be in range from 0.9-0.95, and shall be taken equal to 1.0 for safety. Then Eq. (20) shall be expresses as:

$$M_{cr,f} = \left(1 - \frac{R_{e,3}}{100}\right) * 0.126\, bd^2\sqrt{f_c'} \quad \text{Eq. (21)}$$

The term $\left(d - \frac{a}{2}\right)$ in Eq. 14 refers to the lever arm and could be in range of d to 0.71d when the balanced failure occurs. With safety margin, it shall be taken 0.71d, therefore, $M_{n-hr,fiber}$could be expressed as:

$$M_{n-hr,fiber} = 0.71d\ A_{hr,min}\ f_{hr,bar} \quad \text{Eq. (22)}$$

$$0.71d\ A_{hr,min}\ f_{hr,bar} = \left(1 - \frac{R_{e,3}}{100}\right) * 0.178\ bd^2\sqrt{f_c'} \quad \text{Eq. (23)}$$

$$\rho_{min} = \frac{A_{hr,min}}{bd} = \left(1 - \frac{R_{e,3}}{100}\right)\frac{0.178\sqrt{f_c'}}{f_{hr,bar}} \quad \text{Eq. (24)}$$

According to ACI 318-19, the minimum reinforcement was derived based on M_n/M_{cr} ~1.4, ignoring the effect of beam depth. Therefore, the minimum reinforcement shall be calculated as follows:

$$\rho_{min} = \frac{A_{hr,min}}{bd} = \left(1 - \frac{R_{e,3}}{100}\right)\frac{0.25\sqrt{f_c'}}{f_{hr,bar}} \quad \text{Eq. (25)}$$

Applying the above equation, the minimum reinforcement of the specimens investigated of this study shall be 0.10% of the cross section with factor of safety 1.55.

4.3 Minimum Hybrid Reinforcement Based on the ductility index approach (DI)

According to the load-deflection relationship shown in **Fig. 10**, the ductile response of concrete beams reinforced with hybrid bars and hybrid fibers could be obtained when $P_u > P_{cr}^*$ [44]. The ductile behavior can be defined by the positive value of the ductility index (DI), which is expressed by the following formula [45]:

$$DI = \frac{P_u - P_{cr}^*}{P_{cr}^*} = \frac{M_u - M_{cr}^*}{M_{cr}^*} = \frac{M_u}{M_{cr}^*} - 1 \quad \text{Eq. (26)}$$

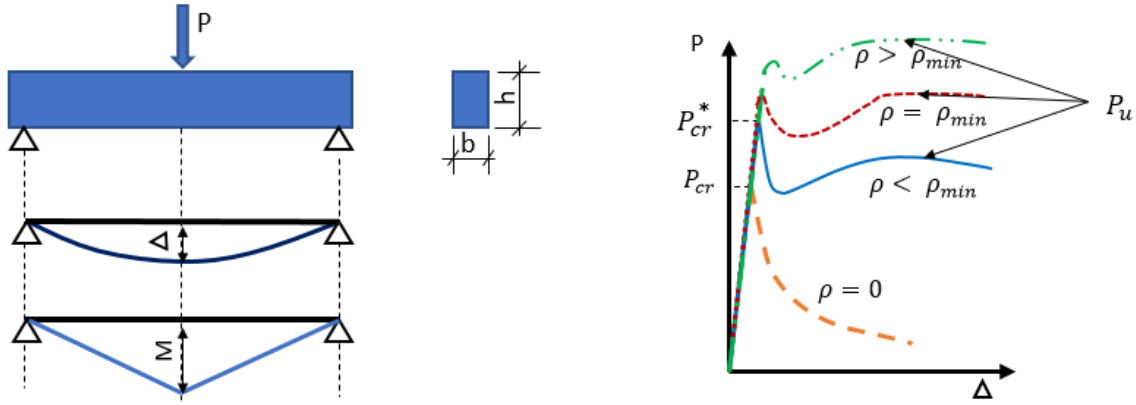

(a) (b)

Fig. 10. The behavior of LRC and FRC beams: (a) three-point bending test; and (b) load-midspan deflection curves.

On the other side, brittle failure occurs when DI has a negative value, which means the beams can't resist any load after the cracking capacity ($P_u < P_{cr}^*$) [44]. Therefore, the definition of minimum reinforcement could be defined by imposing DI equal to zero, and the A_{smin} it could be expressed as follows:

$$A_{smin} = A_s/(DI + 1) \quad \text{Eq. (27)}$$

Substituting by Eq. 23 into Eq. 27, we can get,

$$A_{smin} = A_s/(\frac{M_u}{M_{cr}^*}) \quad \text{Eq. (28)}$$

The cracking moment of hybrid fiber concrete beams (M_{cr}^*) with a rectangular section (b x h) could be computed as follows:

$$M_{cr}^* = \left(1 + \frac{R_{e,3}}{100}\right)\frac{f_r\ b\ h^2}{6} \quad \text{Eq. (29)}$$

The ultimate moment of hybrid fiber concrete beams reinforced with hybrid bars (M_u) could be calculated using the equations provided by the author in Ref. [38].

The DI for RC beams reinforced with the minimum reinforcement area of steel in ACI 318-

19 of beams could be calculated based on the cracking moment of concrete and the flexural capacity of minimum steel reinforcement area. Thus, The DI of fiberless beams with cross sections of 150 x 300 mm and 150 x 450 mm was 0.787 and 0.897, respectively. Moreover, Considering the effect of hybrid fibers, The DI of hybrid fiber concrete with the minimum steel reinforcement ratio with cross sections of 150 x 300 mm and 150 x 450 mm was 0.28 and 0.369, respectively. This could be led to reduce the minimum reinforcement ratio by mean of 62%. **Table 3** shows the results of theoretical and NLFEA. Reference to the same DI obtained for hybrid fiber reinforced concrete with steel bars, the minimum hybrid reinforcement ratios from NLFEA is 0.081for group A as shown in **Fig. 11** and 0.072% for group B as shown in **Fig. 12**. The results revealed that there was a good agreement between theoretical and NLFEA models. Also, the reinforcement ratio versus ductility index curves estimated by theoretical equations is presented in **Fig. 13** and **14**.

Following the definition stated in Eq. (27), the minimum reinforcement of the specimens investigated in this study shall be a function of the volume fraction of the fiber used which not cover in this study and recommended to investigate this parameter in other future study.

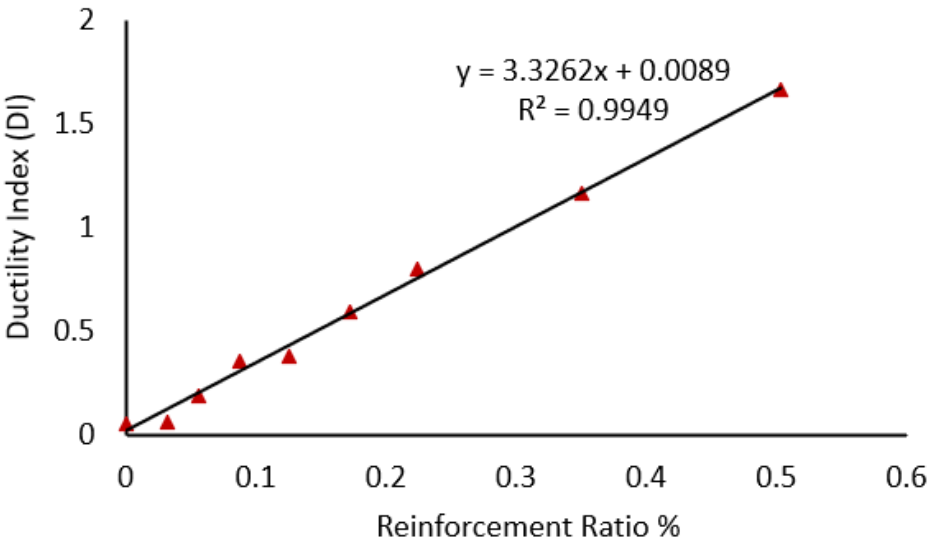

Fig. 11. Relationship between Reinforcement ratio (ρ) and ductility index (DI) of group A based on NLFEA models

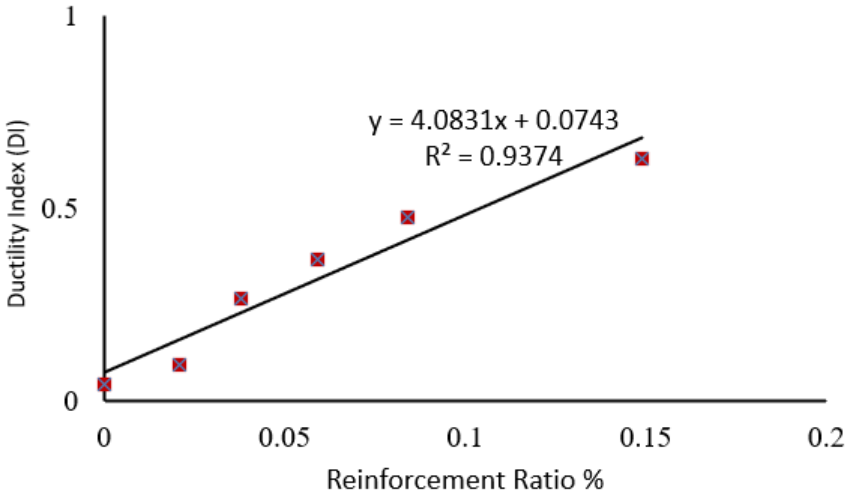

Fig. 12. Relationship between Reinforcement ratio (ρ) and ductility index (DI) of group B based on NLFEA models

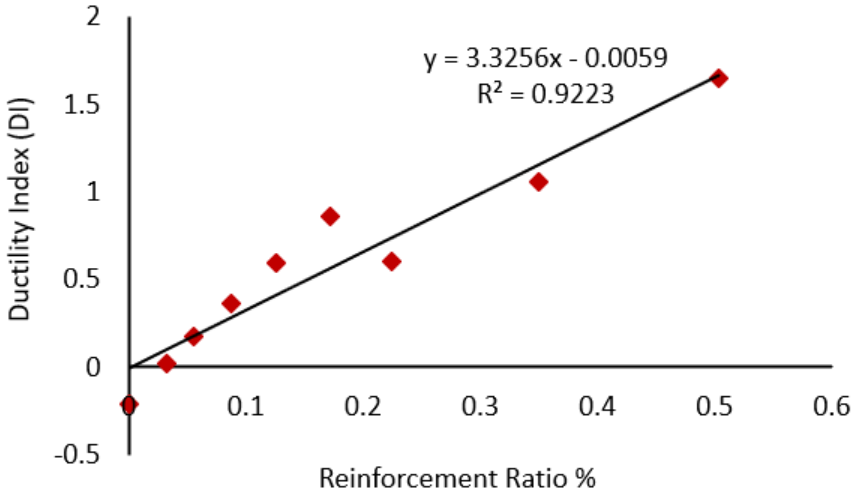

Fig. 13. Relationship between Reinforcement ratio (ρ) and ductility index (DI) of group A based on Theoretical results.

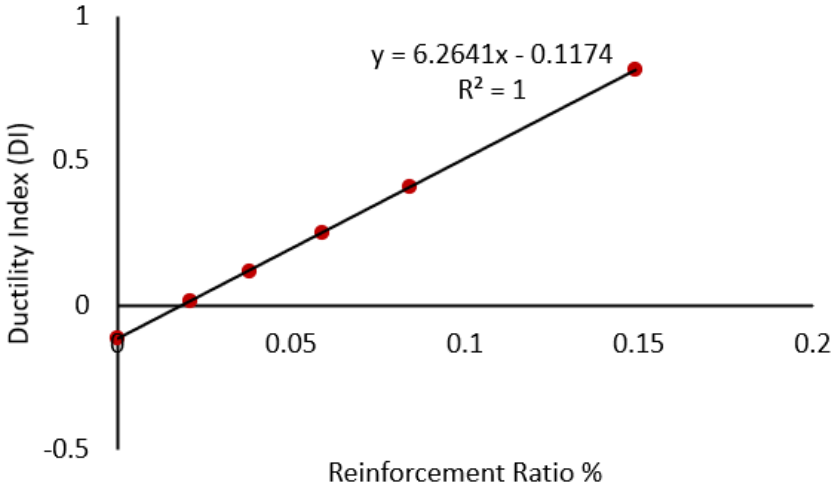

Fig. 14. Relationship between Reinforcement ratio (ρ) and ductility index (DI) of group B based on Theoretical results

Theoretical equations were validated with 34 specimens from other studies as presented in **Table 4**. The comparison shows a good agreement between the theoretical and test results. Furthermore, establishing design procedure that could be used for design of concrete beams reinforced with hybrid reinforcement bars and hybrid polypropylene fibers is presented in **Fig. 15**.

Table 3. Results of NLFEA and comparison with theoretical results

Beam	Geometric Parameters				Bottom RFT.			PP	MS-Fibers			Theoretical results				NLFEA results				Comparison
	b (mm)	h (mm)	L (mm)	X* (mm)	A_{hr} (mm^2)	ρ %	RFT type	V_{PP} %	L_f/d_f	V_{MS} %	L_f/d_f	Mcr* kN.m	M_n kN.m	DI_{TH}	$\rho_{min,Th.}$ %	Mcr* kN.m	M_n kN.m	DI_{NL}	$\rho_{min,NL}$ %	$\frac{\rho_{min,Th.}}{\rho_{min,exp}}$
A1	150	300	2000	800	-	-	hybrid	-	-	-	-	11.64	9.21	-0.209	0.085	54.72	72.72	0.329	0.081	1.05
A2	150	300	2000	800	14.14	0.032	hybrid	3.9	580	3.9	68	11.64	11.9	0.022		9.8	10.368	0.058		
A3	150	300	2000	800	25.14	0.056	hybrid	3.9	580	3.9	68	11.64	13.63	0.171		11.68	12.472	0.068		
A4	150	300	2000	800	39.26	0.088	hybrid	3.9	580	3.9	68	11.64	15.85	0.361		11.784	14.072	0.195		
A5	150	300	2000	800	56.55	0.126	hybrid	3.9	580	3.9	68	11.64	18.55	0.593		11.984	16.248	0.356		
A6	150	300	2000	800	76.96	0.172	hybrid	3.9	580	3.9	68	11.64	21.67	0.861		13.964	19.264	0.38		
A7	150	300	2000	800	100.53	0.224	hybrid	3.9	580	3.9	68	15.71	25.22	0.606		13.964	22.304	0.598		
A8	150	300	2000	800	157.08	0.350	hybrid	3.9	580	3.9	68	16.30	33.51	1.055		14.652	26.364	0.8		
A9	150	300	2000	800	226.19	0.503	hybrid	3.9	580	3.9	68	16.30	43.12	1.645		15.8	34.256	1.169		
B1	150	450	3000	1200	-	-	hybrid	3.9	580	3.9	68	26.20	23.16	-0.116	0.077	16.58	44.168	1.664	0.072	1.07
B2	150	450	3000	1200	14.14	0.021	hybrid	3.9	580	3.9	68	26.20	26.58	0.015		21.6	22.536	0.044		
B3	150	450	3000	1200	25.14	0.037	hybrid	3.9	580	3.9	68	26.20	29.28	0.118		23.46	25.704	0.096		
B4	150	450	3000	1200	39.26	0.058	hybrid	3.9	580	3.9	68	26.20	32.76	0.25		24.06	30.45	0.266		
B5	150	450	3000	1200	56.54	0.083	hybrid	3.9	580	3.9	68	26.20	36.98	0.411		24.66	33.756	0.369		
B6	150	450	3000	1200	100.53	0.14	hybrid	3.9	580	3.9	68	26.20	47.58	0.816		25.806	38.088	0.476		

* refer to the distance from support to the location of applied load.

Table 4. Comparison between theoretical equation used in the study and experimental results of other studies

`Reference	specimen	f'_c (MPA	Geometric			Bottom RFT.			Test Results				Theoretical Results				Compariso
			b (mm)	h (mm)	L (mm	A_s (mm^2	f_y (MPa	ρ_{act}	Mcr* kN.m	M_u kN.m	$DI_{exp.}$	$\rho_{min,Th.}$ %	Mcr* kN.m.	M_n kN.m	DI_{TH}	$\rho_{min,Th.}$ %	$\frac{\rho_{min,Th.}}{\rho_{min,exp}}$
Bosco et al. [46]	A1	75.7	150	100	600	13	637	0.087	1.760	0.832	-0.528	0.315	1.480	0.725	-0.509	0.269	0.853
	A2	75.7	150	100	600	39	569	0.260	1.875	1.690	-0.098		1.702	1.920	0.125		
	A3	75.7	150	100	600	101	441	0.674	2.030	3.310	0.631		2.071	3.81	0.84		
	A4	75.7	150	100	600	157	456	1.047	2.240	7.170	2.201		2.071	6.03	1.913		
	B1	75.7	150	200	1200	20	569	0.067	5.860	1.740	-0.703	0.222	5.917	2.010	-0.660	0.240	1.081
	B2	75.7	150	200	1200	59	569	0.197	6.250	5.140	-0.177		6.116	5.910	-0.032		
	B3	75.7	150	200	1200	151	637	0.504	6.710	17.01	1.536		8.282	16.64	1.009		
	B4	75.7	150	200	1200	236	456	0.787	8.000	22.96	1.870		8.282	19.10	1.306		
	C1	75.7	150	400	2400	25	637	0.042	22.02	5.040	-0.771	0.234	23.665	6.00	-0.746	0.282	1.205
	C2	75.7	150	400	2400	79	569	0.132	23.24	14.64	-0.370		23.66	16.88	-0.286		
	C3	75.7	150	400	2400	201	441	0.335	25.89	39.00	0.507		28.15	33.10	0.177		
	C4	75.7	150	400	2400	314	456	0.524	29.36	58.60	0.996		33.13	53.06	0.602		
Ruiz et al. [47]	A1	39.5	50	75	300	5	538	0.134	0.270	0.210	-0.222	0.182	0.200	0.167	-0.166	0.184	1.010
	A2	39.5	50	75	300	10	538	0.267	0.270	0.375	0.389		0.260	0.330	0.271		
	B1	39.5	50	150	600	5	538	0.067	1.020	0.210	-0.794	0.236	0.801	0.350	-0.563	0.182	0.771
	B2	39.5	50	150	600	10	538	0.134	0.975	0.398	-0.591		0.801	0.710	-0.113		
	B3	39.5	50	150	600	20	538	0.267	1.020	1.200	0.177		1.039	1.390	0.338		
	C1	39.5	50	300	1200	10	538	0.067	3.390	0.45	-0.87	0.187	2.93	1.480	-0.538	0.145	0.775
	C2	39.5	50	300	1200	20	538	0.134	3.390	0.67	-0.81		2.93	2.960	-0.76		
Carpinteri [48]	A1	24.4	150	200	1200	28	489	0.094	3.390	3.030	-0.106	0.122	3.358	2.540	-0.243	0.127	1.040
	A2	24.4	150	200	1200	57	489	0.190	4.230	5.310	0.256		3.536	5.11	0.446		
	B1	24.4	200	800	4800	79	456	0.050	42.240	33.360	-0.210	0.089	71.65	27.87	-0.611	0.128	1.430
	B2	24.4	200	800	4800	157	456	0.099	52.080	54.36	0.044		71.65	55.08	-0.231		
	B3	24.4	200	800	4800	236	456	0.148	54.720	72.7	0.329		71.65	82.32	0.149		
Brinker et al. [49]	A1	98.5	100	100	1200	13	740	0.130	1.050	0.960	-0.085	0.144	1.124	0.840	-0.253	0.194	1.440
	A2	98.5	100	100	1200	25	740	0.250	1.080	1.770	0.639		1.318	1.610	0.221		
Elrakib et al.[50]	A1	43.2	250	400	3300	157	480	0.157	31.020	36.300	0.171	0.134	29.80	28.46	-0.044	0.166	1.238
	A2	43.2	250	400	3300	226	515	0.226	36.710	62.28	0.697		33.56	43.26	0.289		
	B1	60.6	250	400	3300	192	495	0.192	34.422	41.66	0.285	0.141	36.05	35.58	-0.013	0.196	1.390
	B2	60.6	250	400	3300	270	501	0.270	38.032	65.51	0.723		41.11	50.0.5	0.227		
Lange kornbak and karihalo [51]	A1	43.0	100	100	600	13	485	0.130	1.035	0.660	-0.362	0.198	0.744	0.515	-0.307	0.2125	1.073
	A2	43.0	100	100	600	13	485	0.130	1.050	0.720	-0.314		0.744	0.515	-0.307		
	A3	43.0	100	100	600	25	485	0.250	1.050	1.320	0.258		0.869	0.990	0.140		
	A4	43.0	100	100	600	25	485	0.250	1.095	1.380	0.261		0.869	0.99	0.140		

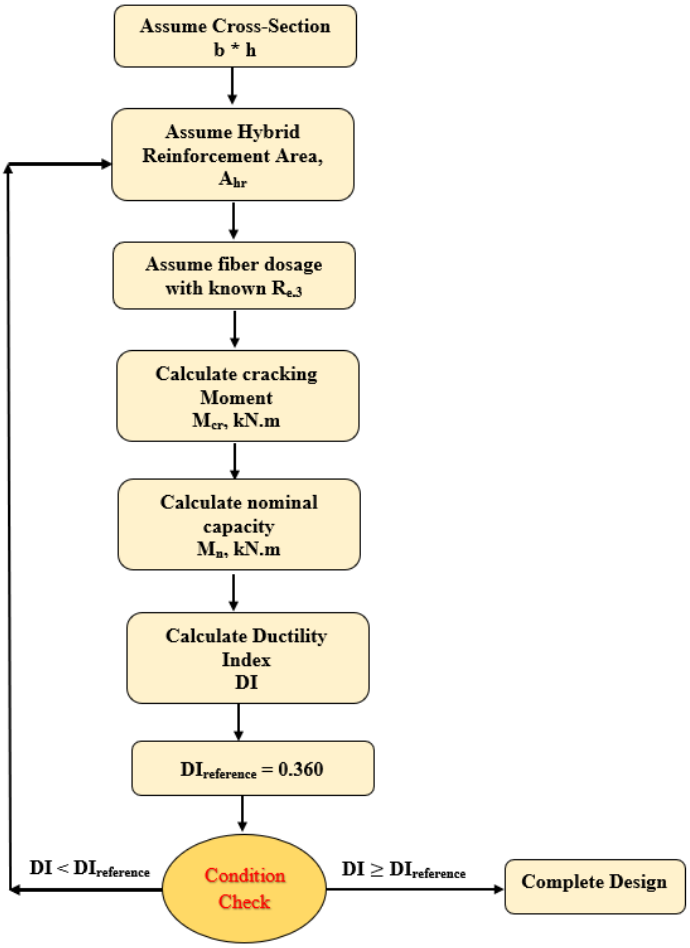

Fig. 15. Design Procedure chart of concrete beam with hybrid fibers and hybrid bars

Conclusions

The goal of this study is to estimate numerically and theoretically the minimum hybrid reinforcement ratio of hybrid fiber concrete beams. Proposed equations are presented for predicting the flexural cracking and nominal strength for concrete beams with hybrid bars and hybrid fibers. Two approaches were reported and analyzed to verify the minimum hybrid reinforcement ratio based on cracking moment and ductility index. In this study, the important conclusions can be summarized as follows:

- The ductility index (DI) could be used to differentiate between the brittle and ductile behavior of concrete beams reinforced with hybrid fibers and hybrid bars in relation to the effective cracking load and ultimate load of a beam
- The minimum hybrid reinforcement, corresponding to DI = 0, is a linear combination of the minimum amount of rebar
- The inclusion of hybrid fibers was effective and helped reduce the required minimum reinforcement ratio by mean of 50%.
- The NLFE model results introduce an acceptable minimum reinforcement ratio by mean of 0.081% and good agreement with the theoretical model.
- The minimum reinforcement ratio obtained using the cracking moment approach is more conservative than that obtained using the ductility index approach.

References

[1] H. Yalciner, A. Kumbasaroglu, A. K. El-Sayed, A. P. Balkıs, E. Dogru, A. I. Turan, A. Karimi, R. Kohistani, M. F. Mermit, and K. Bicer, Flexural Strength of Corroded Reinforced Concrete Beams, ACI Structural Journal, V. 117, No. 1, January 2020.

[2] J. Cai, J. Pan, X. Zhou, Flexural Behavior of Basalt FRP reinforced ECC and Concrete Beams, Construction and Building Materials, 142 (2017) 423-430.

[3] J. Plecnik and S. H. Ahmad. Transfer of composite technology to design and construction of bridges. Final report to US DOT, contract no. DTRS 5683-C000043 (1988).

[4] ACI Committee 440. Report on fiber-reinforced polymer (FRP) reinforcement for concrete structures. ACI 440R -07, American Concrete Institute, Farmington Hills, MI (2007).

[5] A. Nanni. Composites: Coming on strong. Concrete Construction 44 (1): 120–124 (1999).

[6] SINTEF Report STF22 A98741. Modifications to NS3473 when using fiber reinforced plastic reinforcement 2.24. Norwegian Council for Building Standardization, Oslo, Norway (2002).

[7] A. K. Kaw. Mechanics of composite materials, 2nd ed. Boca Raton, FL: Taylor and Francis (2005).

[8] D. W. Seo, K. T. Park, Y.J. You, and S. Y. Lee, Experimental Investigation for Tensile Performance of
GFRP-Steel Hybridized Rebar, Advances in Materials Science and Engineering, (2016), 9401427.

[9] J. Cai, J. Pan, X. Zhou, Flexural Behavior of Basalt FRP reinforced ECC and Concrete Beams, Construction and Building Materials, 142 (2017) 423-430.

[10] M. Mirdarsoltany, A. Rahai, F. Hatami, R. Homayoonmehr, and F. Abed, Investigating Tensile Behavior of Sustainable Basalt–Carbon, Basalt–Steel, and Basalt–Steel-Wire Hybrid Composite Bars, MDPI Sustainability 2021, 13, 10735.

[11] T. A. El-Sayed, A. M. Erfan, R. M. Abdelnaby, and M. K. Soliman, Flexural behavior of HSC beams reinforced by hybrid GFRP bars with steel wires, Case Studies in Construction Materials 16 (2022) e01054.

[12] W. Qu, X. Zhang, H. Huang, Flexural Behavior of Concrete Beams Reinforced with Hybrid (GFRP and Steel) Bars, Journal of Composites for Constructions, 13 (5) (2009) 350-359.

[13] A. Bentur and S. Mindess, Fiber Reinforced Cementitious Composites, Modern Concrete Technology Series, Taylor & Francis.

[14] R.J. Craig, J. Decker, L. Dombrowski, Jr R. Laurencelle and J. Federovich, 'Inelastic behavior of reinforced fibrous concrete', J. Struct. Eng. ASCE 113, 1987, 802–817.

[15] T. Y. Lim, P. Paramasivam and S. L. Lee, 'Behaviour of reinforced steel fiber concrete beams in flexure', J. Struct. Eng. ASCE 113, 1987, 2439–2458.

[16] T. Kanazu, Y. Aoyagi and T. Nakano, 'Mechanical behavior of concrete tension members reinforced with deformed bars and steel fiber', Trans. Japan Concrete Institute. 4, 1982, 395–402.

[17] E. S. Bernard, Effect of synthetic fibers and aggregate size on flexural crack widths', ACI Structural Journal, V. 116, No. 3, may 2019, pp. 677-686.

[18] N. Buratti, C. Mazzotti, and M. Savoia, Post-cracking behavior of steel and macro-synthetic fiber-reinforced concretes, Construction and Building Materials, 25, 2011, 2713-2722.

[19] M. G. Alberti, A. Enfedaque and J. C. Gálvez, Improving the Reinforcement of Polyolefin Fiber Reinforced Concrete for Infrastructure Applications, Fibers, 2015, 504-522.

[20] Sahoo, D. R.; Solanki, A.; and Kumar, A., "Influence of Steel and Polypropylene Fibers on Flexural Behavior of RC Beams," Journal of Materials in Civil Engineering, ASCE, V. 27, No. 8, 2014, p. 04014232

[21] A. Abbadi, P.A.M. Basheer, J. P. Forth, Effect of hybrid fibers on the static load performance

of concrete beams, Materials Today: Proceedings, 65 (2022), 681-687.
[22] B. Chiaia, A. P. Fantilli, and P. Vallini, Evaluation of minimum reinforcement ratio in FRC members and application to tunnel linings, Materials and Structures (2007), 593–604.
[23] M. Gümüş and A. Arslan, "Effect of fiber type and content on the flexural behavior of high strength concrete beams with low reinforcement ratios", Structures, 2019, 1:10.
[24] ACI Committee 318. Building code requirements for structural concrete (ACI 318-08) and commentary (ACI 318R-08). MI: Farmington Hills; 2008.
[25] European Committee for Standardization, Eurocode 2: Design of Concrete Structures, Part 1-1, General Rules and Rules for Buildings, Brussels, Belgium, 2004.
[26] Canadian Standards Association, "Design of concrete structures," (CSA A23.3-04), 2004.
[27] M. Bruckner and R. Eligehausen, "Minimum reinforcement in RC beams," in Proceedings of the 2nd International PhD Symposium in Civil Engineering, pp. 135–141, Budapest, Hungary, May 1998.
[28] Bazant, Z.P. (1987). "Snapback instability at crack ligament tearing and its implication for fracture micromechanics, "Cement and Concrete Research 17, pp. 951-967.
[29] Bosco, C., and Carpinteri, A. (1992). 'Fracture mechanics evaluation on minimum reinforcement in concrete structures," Application of Fracture Mechanics to Reinforced Concrete, Ed. by A. Carpinteri, Elsevier Applied Science, Torino, Italy, pp. 347-377.
[30] Bigaj, A., and Walraven, J.C. (1993). "Size effect on the rotational capacity of plastic hinges in reinforced concrete beams", CEB-Bulletin 218.
[31] Carpinteri, A. (1981). "A fracture mechanics model for reinforced concrete collapse," IABSE Colloquium on Advanced Mechanics of Reinforced Concrete, Delft, pp. 17-30.
[32] J. Ozbolt and M. Bruckner, Minimum Reinforcement Requirement for RC Beams. European Structural Integrity Society, V. 24, 1999, pp. 181-201.
[33] Fantilli, A.P.; Chiaia, B.; Gorino, A. Fiber volume fraction and ductility index of concrete beams. Cem. Concr. Compos. 2016, 65, 139–149.
[34] Liao, L.; de la Fuente, A.; Cavalaro, S.; Aguado, A. Design of FRC tunnel segments considering the ductility requirements of the Model Code 2010. Tunn.Undergr. Space Technol. 2015, 47, 200–210.
[35] Naaman, A.E. Strain hardening and deflection hardening fiber reinforced cement composites. In Proceedings of the 4th International RILEM Workshop on High Performance Fiber Reinforced Cement Composites, University of Michigan, Ann Arbor, MI, USA, 16–18 June 2003; pp. 95–113.
[36] Chiaia, B.; Fantilli, A.P.; Vallini, P. Combining fiber-reinforced concrete with traditional reinforcement in
tunnel linings. Eng. Struct. 2009, 31, 1600–1606.
[37] Liao, L.; de la Fuente, A.; Cavalaro, S.; Aguado, A. Design procedure and experimental study on fiber
reinforced concrete segmental rings for vertical shafts. Mater. Des. 2016, 92, 590–601.
[38] A.H. Abd El-Karim, G. I. Khalil, A.E. Ewis, and M. H. Makhlouf, Impact of developed hybrid polypropylene fiber inclusion on the flexural performance of concrete beams reinforced with innovative hybrid bars, Construction and Building Materials, 409 (2023), 134113.
[39] J.G. MacGregor, Reinforced Concrete Mechanics and Design, Prentice-Hall, Inc., Englewood Cliffs, NJ, 1992.
[40] S.M. Iqbal, S. Zainal, F. Hejazi, F.N.A. Abd. Aziz and M.S. Jaafar, Constitutive Modeling of New Synthetic Hybrid Fibers Reinforced Concrete from Experimental Testing in Uniaxial Compression and Tension, MDPI (Crystal), 10 (2020) 885.
[41] Kent, D.C.; Park, R. Flexural Members with Confined Concrete. J. Struct. Eng. Div. 1971, 97, 1969–1990.

[42] F. Legeron and P. Paultre, Prediction of Modulus of Rupture of Concrete, ACI Materials Journal, V. 97 (2000), pp. 193-200.

[43] EN 14651, "Test Method for Metallic Fibred Concrete – measuring the flexural Tensile Strength (Limit of proportionality [LOP], Residual), British Standard Institution, V.3, 2005, pp. 1-17.

[44] A. P. Fantilli, B. Chiaia, and A. Gorino, Unified Approach for Minimum Reinforcement of Concrete Beams, ACI Structural Journal, V. 113, 2016, pp 1107-1116.

[45] Fantilli, A. P.; Gorino, A.; and Chiaia, B., "Precast Plates Made with Lightweight Fiber-Reinforced Concrete," Proceedings of the FRC 2014 Joint ACI-fib International Workshop, Montreal, QC, Canada, 24-25 July 2014, pp. 224-234.

[46] C. Bosco, A. Carpinteri, and P. G. Debernardi, Minimum Reinforcement in High-Strength Concrete, J. Struct. Eng. 1990.116:427-437.

[47] Ruiz, G.; Elices, M.; and Planas, J., "Size Effect and Bond-Slip Dependence of Lightly Reinforced Concrete Beams," European Structural Integrity Society, V. 24, 1999, pp. 67-97.

[48] Carpinteri, A., "Minimum Reinforcement in Reinforced Concrete Beams," RILEM TC 90-FMA, Code Work, Cardiff, UK, Sept. 1989.

[49] Brincker, R.; Henriksen, M. S.; Christensen, F. A.; and Heshe, G., "Size Effects on the Bending Behaviour of Reinforced Concrete Beams," European Structural Integrity Society, V. 24, 1999, pp. 127-137.

[50] Elrakib, T. M., "Performance Evaluation of HSC Beams with Low Flexural Reinforcement," HBRC Journal, V. 9, Apr. 2013, pp. 49-59.

[51] Lange-Kornbak, D., and Karihaloo, B. L., "Fracture Mechanical Prediction of Transitional Failure and Strength of Singly-Reinforced Beams," European Structural Integrity Society, V. 24, 1999, pp. 31-66.